

Exchange Effects on the Electron and Hole Mobility in Crystalline Anthracene and Naphthalene

ROBERT SILBEY,* JOSHUA JORTNER, STUART A. RICE, AND MARTIN T. VALA, JR.†

Department of Chemistry and Institute for the Study of Metals, The University of Chicago, Chicago, Illinois

(Received 14 September 1964)

In this paper we present the results of calculations of the electron and hole band structure of crystalline anthracene and naphthalene in the tight binding approximation, and of the mobility tensor in the constant-free-time and constant-free-path approximations. This treatment differs from previous formulations by inclusion of the effects of intermolecular electron exchange and of vibronic coupling (in the weak coupling scheme). The bandwidths were found to be of the order of 0.02 eV and smaller, and the mobility data were found to be consistent with the band scheme. The predicted mobility in the c' direction is found to be in good agreement with experiment, in contrast to previous treatments.

I. INTRODUCTION

THE experimental work of Kepler,¹ of LeBlanc,² and of Thaxton, Jarnagin, and Silver³ on the mobilities of excess electrons and holes in crystalline anthracene has shown that: (i) the mobilities are slightly anisotropic and of the order of magnitude of 1 cm²/sec·V at room temperature, and (ii) the mobilities vary with temperature as T^{-n} with n between 1 and 2. A mechanism of charge-carrier transport that involves phonon-assisted hopping from molecule to molecule would imply that the carrier mobility increases with temperature; this is contrary to experiment. On the other hand, a simple band scheme is consistent with experiment. This fact led LeBlanc⁴ to attempt a calculation of the excess electron and hole band structures and the mobilities of excess charge carriers in crystalline anthracene using the following assumptions: (a) the crystal is rigid and composed of nonvibrating molecules, (b) the wavefunction of the excess electron or hole may be represented by a Bloch sum of molecular orbitals, (c) the molecular orbitals are linear combinations (Hückel) of single Slater carbon-atom $2p$ orbitals, (d) intermolecular overlap may be neglected, (e) the potential of a neutral molecule may be taken as the Goepfert-Mayer and Sklar potential, and (f) only two-center integrals need be considered. With these assumptions, LeBlanc was able to obtain order-of-magnitude agreement with the experimental observations.

Katz, Choi, Rice, and Jortner⁵ extended this calculation, improving on (c), (d), and (f). The analysis properly accounts for the fact that anthracene has two molecules per unit cell by constructing symmetry adapted functions. The best available⁶ SCF atomic

orbitals for carbon were used in the calculation of the necessary integrals, and many three-center terms were computed. With these improvements, Katz *et al.* obtained fairly good agreement between the predicted mobility ratios and the experimental data. Now, the mobilities cited above were computed assuming either the constant free time or the constant free path models. From a combination of the experimental data and their calculated mobilities, Katz *et al.* find a free path of ~ 4 Å, which is very close to the lattice spacing in anthracene. This mean free path is so short that the applicability of the band model to this system may be questioned. Another serious point in the above calculations is that the calculated mobilities in the c' direction are very much smaller than those in the other directions, contrary to experimental data.

In the present work, the calculations of Katz, Choi, Rice, and Jortner are extended further as follows:

(a) The effect of molecular vibrations is included by taking the molecular wavefunctions as the product of an electronic part and a vibrational part. This representation corresponds to the weak-coupling limit of vibronic interaction, i.e., the nuclear part of the Hamiltonian is diagonalized before the crystal field part. Using this approximation, the symmetrized wavefunctions of the *crystal* with an excess or deficiency of one electron may be written in the form

$$\Psi_{\pm}(\mathbf{K}) = \sum_{l=0}^{2N-1} (\pm 1)^l \exp(i\mathbf{K} \cdot \mathbf{r}_l) \alpha \phi_l^k(1) \times \prod_{i=0}^{2N-1} (\phi_i'(i, 1) \cdots \bar{\phi}_i^{\beta}(i, 2a) \chi_i), \quad (1)^7$$

where ϕ^k is the lowest unoccupied molecular orbital of a molecule for electrons and the highest occupied orbital for holes, the ϕ_i are the a occupied molecular orbitals of Molecule i , the bar over ϕ_i^{β} means that the electron in that molecular orbital has β spin, and χ_i is the ground-state vibrational wavefunction of the i th molecule. It is assumed that all the vibrational wavefunctions are the same except for that of the molecule

⁷ There are two possible wavefunctions for electrons, as well as holes, due to the two inequivalent molecules per unit cell. These are represented as Ψ_+ and Ψ_- . N is the number of unit cells.

* NSF Cooperative Fellow.

† NIH Fellow.

¹ (a) R. G. Kepler, Phys. Rev. **119**, 1226 (1960). (b) R. G. Kepler, Org. Semicond. Proc. Inter-Ind. Conf. 1962, 1 (1962).

² O. H. LeBlanc, J. Chem. Phys. **33**, 626 (1960).

³ G. D. Thaxton, R. C. Jarnagin, and M. Silver, J. Phys. Chem. **66**, 2461 (1962).

⁴ O. H. LeBlanc, J. Chem. Phys. **35**, 1275 (1961).

⁵ J. L. Katz, S. I. Choi, S. A. Rice, and J. Jortner, J. Chem. Phys. **39**, 1683 (1963).

⁶ P. S. Bagus, T. L. Gilbert, C. C. J. Rootaahn, and H. D. Cohen "Analytic SCF Functions for the First Row Atoms," (to be published). The atomic orbitals used is the $2p\pi$ of the 3P state of atomic carbon.

with an excess electron (or hole). This formalism implies, of course, that every electron or hole band is split into many bands, each characterized by a vibrational wavefunction. The $\mathbf{K}=0$ levels of these bands will be separated by the vibrational quantum, which in aromatic molecules is of the order of 0.2 eV. It is seen later that the bandwidths are of the order of 0.01 eV and thus the bands are well separated.

(b) The potential of the n th neutral molecule was taken previously to be the Goepfert-Mayer and Sklar potential (or Hartree potential):

$$V_n'(\mathbf{r}-\mathbf{r}_n) = -\sum_A (Ze^2/R_A) + 2\sum_{i=0}^a J_n^i, \quad (2)$$

where R_A is the distance from the A th nucleus of the n th molecule to the electron, and J_n^i is the Coulomb potential of the i th molecular orbital of the n th molecule. Instead of this potential, the following potential is used herein:

$$\begin{aligned} V_n(\mathbf{r}-\mathbf{r}_n) &= -\sum_A (Ze^2/R_A) + \sum_{i=0}^a (2J_n^i - K_n^i) \\ &= V_n'(\mathbf{r}-\mathbf{r}_n) - \sum_{i=0}^a K_n^i, \end{aligned} \quad (3)$$

where K_n^i is the exchange potential of the i th molecular orbital on the n th molecule.

It should be emphasized that in the present analysis we are solving the problem by considering the wavefunction of the entire crystal, while previous work considered only the wavefunction of the excess electron or hole.

II. NUMERICAL CALCULATIONS

The Hamiltonian of the crystal may be written as the sum of two terms, the first of which contains all contributions that refer to the lone electron (H'), and the second of which is the remainder ($H-H'$). The energy of the crystal, neglecting overlap between molecules, may be written as

$$E_{\pm}(\mathbf{K}) = \varepsilon_0 + \sum_i (\pm 1)^i [\cos(\mathbf{K} \cdot \mathbf{r}_i)] \varepsilon_i, \quad (4)$$

where

$$\varepsilon_0 = \langle \phi_0^k | H' | \phi_0^k \rangle,$$

and

$$\varepsilon_i = \langle \phi_0^k | V_i(\mathbf{r}-\mathbf{r}_i) | \phi_i^k \rangle | \langle \chi' | \chi^0 \rangle|^2. \quad (5)$$

In Eq. (5) χ' represents the vibrational wavefunction of the positive or negative ion and χ^0 that of the neutral molecule.

Replacing V_n by

$$V_n' - \sum_{i=0}^a K_n^i,$$

one finds:

$$\begin{aligned} \varepsilon_i &= | \langle \chi' | \chi^0 \rangle|^2 \langle \phi^k(\mathbf{r}-\mathbf{r}_i) | V_i' - \sum_{i=0}^a K_i^i | \phi^k(\mathbf{r}) \rangle \\ &= | \langle \chi' | \chi^0 \rangle|^2 \{ \langle \phi^k(\mathbf{r}-\mathbf{r}_i) | V_i' | \phi^k(\mathbf{r}) \rangle \\ &\quad - \sum_{i=0}^a \langle \phi^k(\mathbf{r}-\mathbf{r}_i | K_i^i | \phi^k(\mathbf{r}) \rangle \}. \end{aligned} \quad (6)$$

The first term in brackets is that calculated previously,⁵ and the second term is a sum of hybrid integrals. For numerical computation the molecular orbitals were taken to be linear combinations of atomic orbitals; the coefficients used were either Hückel coefficients or Hoyland-Goodman SCF coefficients.⁸ The difference between the results using these two sets is small, and we report only the results for Hückel coefficients. The second term in the brackets, when expanded in atomic orbitals, becomes

$$\sum_{i=0}^a \sum_{\alpha, \beta, \gamma, \delta}^M c_{\alpha}^k c_{\beta}^k c_{\gamma}^i c_{\delta}^i \langle u_{\alpha} u_{\gamma} | 1/r_{12} | u_{\delta} u_{\beta} \rangle, \quad (7)$$

where α, γ, δ number the atoms of Molecule l and β the atoms of the reference molecule. Including only two center terms ($\alpha=\gamma=\delta$) we find:

$$\begin{aligned} &\sum_{i=0}^a \langle \phi^k(\mathbf{r}-\mathbf{r}_i) | K_i^i | \phi^k(\mathbf{r}) \rangle \\ &= \sum_{i=0}^a \sum_{\alpha, \beta}^M c_{\alpha}^k (c_{\alpha}^i)^2 c_{\beta}^k \langle u_{\alpha} u_{\alpha} | u_{\alpha} u_{\beta} \rangle, \end{aligned} \quad (8)$$

where the index representing the molecule has been

TABLE I. Hybrid sums (units 10^{-2} eV).

Molecule coordinates in a, b, c space ^a	$\sum_{i=1}^a \langle \phi_0^k K_n^i \phi_n^k \rangle^b$		$\sum_{i=1}^a \langle \phi_0^{k-1} K_n^i \phi_0^{k-1} \rangle$	
	Naphthalene	Anthracene	Naphthalene	Anthracene
(0, 0, 1)	-0.8033	0.5806	-0.2555	0.1953
(0, 1, 0)	0.6641	1.933	-4.412	-4.451
(0, 1, 1)	0.0096	0.0073	-0.0923	-0.1391
(1, 0, 0)	-0.0045	0.0133	0.0156	0.0089
(1, 0, 1)	0.0822	-0.0502	0.3824	-0.1547
(1, 1, 0)	-0.0027	0.0029	0.0241	0.0043
(1, 1, 1)	-0.0023	0.0018	0.0099	-0.0015
($\frac{1}{2}$, $\frac{1}{2}$, 0)	-1.236	-2.550	1.337	-1.261
($\frac{1}{2}$, $\frac{1}{2}$, 1)	0.1704	-0.0743	-0.8940	0.8477
($-\frac{1}{2}$, $\frac{1}{2}$, 1)	-0.0020	0.0019	-0.0011	0.0005
(-1, 0, 1)	0.0	0.0	0.0	0.0
(-1, 1, 1)	0.0	0.0	0.0	0.0
($\frac{1}{2}$, $\frac{3}{2}$, 0)	0.0002	0.0011	0.0085	-0.0001

^a This gives the vector to the center of the molecule, the unit vectors being the lattice vectors of the crystals in the corresponding directions.

^b In these, k represents the lowest unfilled orbital of the molecule.

⁸ J. R. Hoyland and L. Goodman, J. Chem. Phys. **36**, 12 (1962).

TABLE II. Components of the mobility tensor in constant-free-time-and constant-free-path approximations for various vibrational overlaps.

	Naphthalene					Anthracene				
	I	II	III	IV	V	I	II	III	IV	V
	Hole									
$\langle V_a^2 / V \rangle^a$	0.07	0.5	1.1	1.9	7.3	4.2	0.2	0.4	0.6	3.7
$\langle V_b^2 / V \rangle^a$	9.6	3.8	7.4	10.9	26.1	9.5	3.6	7.1	10	25.7
$\langle V_c^2 / V \rangle^a$	1.5	0.3	0.7	1.1	5.5	1.3	0.5	1.1	1.7	7.6
$\langle V_a V_c / V \rangle^a$	0.2	0.03	0.09	0.2	2.0	0.4	0.1	0.2	0.4	2.1
	Electron									
$\langle V_a^2 / V \rangle^a$	4.5	0.6	1.3	1.9	6.8	8.8	1.2	2.4	3.7	12.6
$\langle V_b^2 / V \rangle^a$	3.0	0.4	0.8	1.3	5.2	5.7	1.3	2.6	4.1	14.2
$\langle V_c^2 / V \rangle^a$	0.1	0.7	1.5	2.1	5.9	0.04	0.5	0.9	1.3	3.5
$\langle V_a V_c / V \rangle^a$	0.04	-0.4	-0.8	-1.2	-4.1	0.01	-0.2	-0.5	-0.7	-2.4
	Hole									
$\langle V_a^2 \rangle^b$	9	2.1	9.4	22.6	255	79	0.6	2.8	6.8	116
$\langle V_b^2 \rangle^b$	146	21.3	85	186.5	1384	191	19	75	163	1274
$\langle V_c^2 \rangle^b$	18	1.2	5	12.6	178	21	1.8	7.8	19	249
$\langle V_a V_c \rangle^b$	2	0.1	1	2.6	74	8	0.4	1.9	4.9	78
	Electron									
$\langle V_a^2 \rangle^b$	42	1.3	5.5	12.5	148	163	4.1	17	39	13
$\langle V_b^2 \rangle^b$	26	0.8	3.1	7.3	96	107	4.4	18	43	14
$\langle V_c^2 \rangle^b$	0.8	1.5	5.7	12.6	117	0.3	1.3	5.1	11	3
$\langle V_a V_c \rangle^b$	-0.5	-0.9	-3.6	-8.2	-95	0.04	-0.9	-3.7	-8.4	-2

^a Constant-free-path approximation units 10^{-6} cm sec⁻¹. I, Taken from Katz *et al.*⁵; II, vibrational overlap squared=0.1; III, vibrational overlap squared=0.2; IV, vibrational overlap squared=0.3; V, vibrational overlap squared=1.0.

^b Constant-free-time approximation units 10^{10} cm² sec⁻².

TABLE III. Widths of excess electron and hole bands in anthracene and naphthalene (units= 10^{-2} eV).^a

Direction	Naphthalene						Anthracene					
	Hole			Electron			Hole			Electron		
	I	II	III	I	II	III	I	II	III	I	II	III
a^+	0.35	0.70	3.5	0.17	0.35	1.7	0.04	0.07	0.18	0.60	1.20	6.0
a^-	0.07	0.13	0.7	0.22	0.43	2.2	0.13	0.26	0.96	0.58	1.16	5.8
b^+	1.22	2.44	12.1	0.06	0.11	0.6	1.35	2.70	14.2	0.17	0.35	1.7
b^-	1.61	3.22	16.1	0.37	0.74	3.7	1.51	3.03	15.3	1.09	2.18	10.9
c^+	0.49	0.98	4.9	0.11	0.23	1.2	0.40	0.81	4.0	0.15	0.31	1.5
c^-	0.43	0.85	4.3	0.43	0.86	4.3	0.57	1.14	5.6	0.29	0.58	2.9

^a I, Vibrational overlap squared=0.1; II, vibrational overlap squared=0.2; III, vibrational overlap squared=1.0.

TABLE IV. Ratios of components of mobility tensor in constant-free-time and constant-free-path approximations.

Naphthalene											
	I		II		III		IV		V		VI
	a	b	a	b	a	b	a	b	a	b	c
Hole											
μ_{aa}/μ_{bb}	0.06	0.07	0.18	0.28	0.10	0.14	0.11	0.15	0.12	0.17	0.64
$\mu_{c'c'}/\mu_{bb}$	0.12	0.16	0.13	0.21	0.06	0.08	0.06	0.09	0.07	0.10	0.29
$\mu_{c'c'}/\mu_{aa}$	2.0	2.1	0.70	0.75	0.55	0.59	0.55	0.58	0.56	0.59	0.44
Electron											
μ_{aa}/μ_{bb}	1.6	1.5	1.5	1.3	1.8	1.6	1.8	1.5	1.7	1.5	1.0
$\mu_{c'c'}/\mu_{bb}$	0.03	0.04	1.2	1.1	1.9	1.8	1.8	1.7	1.7	1.6	0.57
$\mu_{c'c'}/\mu_{aa}$	0.02	0.03	0.8	0.9	1.1	1.2	1.0	1.1	1.0	1.1	0.57

Anthracene											
	I		II		III		IV		V		VI
	a	b	a	b	a	b	a	b	a	b	c
Hole											
μ_{aa}/μ_{bb}	0.41	0.45	0.09	0.14	0.03	0.05	0.04	0.05	0.04	0.06	0.5
$\mu_{c'c'}/\mu_{bb}$	0.11	0.14	0.19	0.30	0.10	0.14	0.11	0.15	0.11	0.17	0.4
$\mu_{c'c'}/\mu_{aa}$	0.26	0.31	2.2	2.1	2.9	3.1	2.8	3.0	2.8	2.8	0.8
Electron											
μ_{aa}/μ_{bb}	1.5	1.5	0.89	0.89	0.92	0.93	0.91	0.92	0.90	0.91	1.7
$\mu_{c'c'}/\mu_{bb}$	0.0	0.01	0.21	0.25	0.30	0.38	0.28	0.35	0.26	0.33	0.4
$\mu_{c'c'}/\mu_{aa}$	0.0	0.01	0.23	0.28	0.32	0.41	0.30	0.38	0.29	0.36	0.24

^a Constant-free-time.
^b Constant-free-path. I, values from Katz *et al.*⁴; II, present paper with vibrational overlap squared=1.0; III, present paper with vibrational overlap squared=0.1; IV, present paper with vibrational overlap squared=0.2; V, present paper with vibrational overlap squared=0.3; VI, experimental values.
^c See Refs. 1-3.

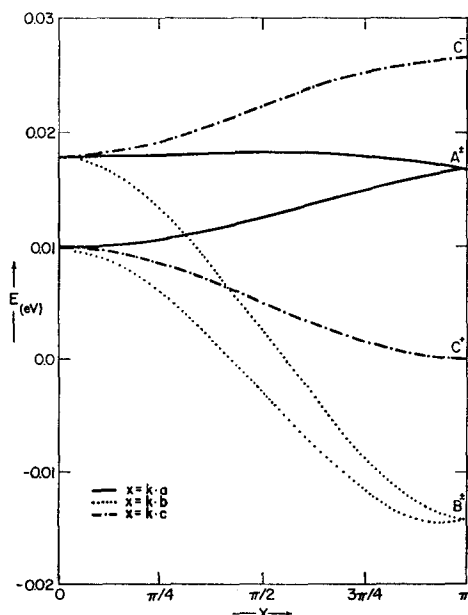


FIG. 1. Shape of excess hole band of naphthalene in the a^{-1} , b^{-1} , c^{-1} directions for vibrational overlap of $(0.2)^{\frac{1}{2}}$.

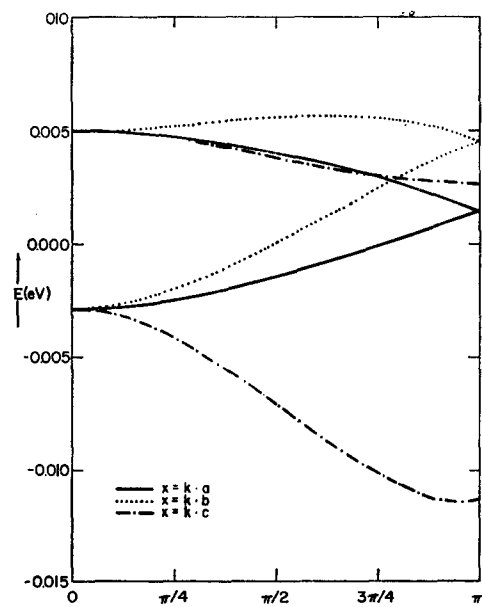


FIG. 2. Shape of excess electron band of naphthalene in the a^{-1} , b^{-1} , c^{-1} directions for vibrational overlap² of $(0.2)^{\frac{1}{2}}$.

suppressed. Since

$$\sum_{i=0}^a (c_i)^2 = \frac{1}{2}$$

by the Coulson-Rushbrooke theorem, we have finally

$$\sum_{i=0}^a \langle \phi^k(\mathbf{r}-\mathbf{r}_i) | K_i^i | \phi^k(\mathbf{r}) \rangle = \frac{1}{2} \sum_{\alpha=1}^M \sum_{\beta=1}^M c_{\alpha}^k c_{\beta}^k \langle u_{\alpha} u_{\beta} | u_{\alpha} u_{\beta} \rangle. \quad (9)$$

These integrals were computed on an IBM 7094 using the same Hartree-Fock SCF carbon atomic wavefunctions as earlier.⁵ The hybrid sums for the 13 molecules considered⁵ are listed in Table I. Using these values in Eq. (4), we have recalculated the band structures and mobilities of the excess hole and electron in anthracene and naphthalene for various values of the vibrational overlap.⁹ The mobilities were computed in both the constant-free-time approximation and the constant-free-path approximation. All results are listed in Tables II, III, and IV and Figs. 1 through 4.

III. CONCLUSIONS

While the components of the mobility tensor cannot be found without making an assumption for the free time or free path, the ratios of these components may be computed without such an assumption. These results are listed in Table IV along with those of the previous

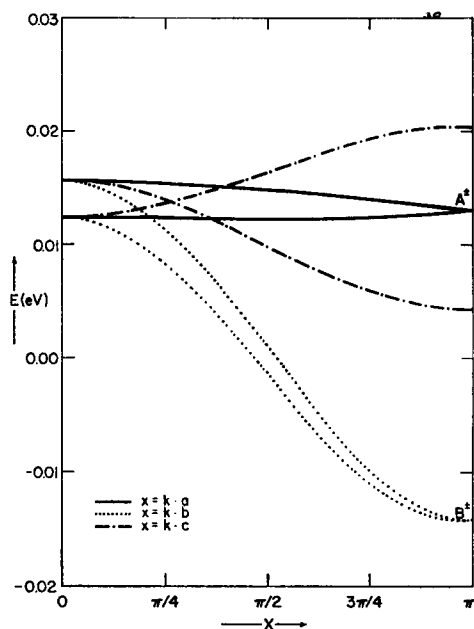


FIG. 3. Shape of excess hole band of anthracene in the a^{-1} , b^{-1} , c^{-1} directions for vibrational overlap of $(0.2)^{\frac{1}{2}}$.

⁹ Let the reader note that the components of the mobility tensor were calculated in the manner of Katz *et al.*⁵, that is the velocity components were averaged over the Boltzmann distribution of electrons in the band. Therefore, although each ϵ_i is modified by the same vibrational overlap, the bandwidth (which is dependent on the vibrational overlap) appears in the exponent of the Boltzmann factor and modifies the integral. Thus only when the Boltzmann factor is close to unity for the entire band will the vibrational overlap factors cancel in the ratio of mobility components. (See Ref. 5, Eq. 35.)

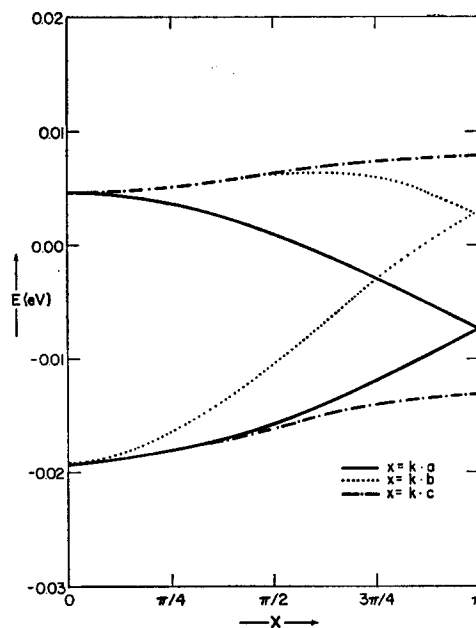


FIG. 4. Shape of excess electron band of anthracene in the a^{-1} , b^{-1} , c^{-1} directions for vibrational overlap of $(0.2)^{\frac{1}{2}}$.

calculation. It may be seen that for a vibrational overlap of ~ 0.5 , for example, the present results are slightly better than the previous results, and the agreement between calculation and experiment is fairly good. The most striking change in the predictions is that the electron mobility in the c' direction has increased an order of magnitude in both anthracene and naphthalene. This prediction is now in very good agreement with experiment. None of the previous calculations resulted in appreciable electron mobility in the c' direction.

The calculated bandwidths are given in Table III. These are smaller than those calculated by Katz *et al.*⁵ and closer to those of LeBlanc for a vibrational overlap of 0.5. It can be seen that the bandwidths are of the order of 0.02 eV and smaller.

From the calculated components of the mobility tensor and the experimental data, one may estimate the free time and the mean free path of the electrons and holes. Katz *et al.*⁵ found the mean free path to be ~ 4 Å for electrons and holes, which is of the order of magnitude of the lattice spacing. The results reported herein for vibrational overlap of 0.5 give a mean free path of the order of 10 Å. The calculated free time is such that the bandwidths are of the order of \hbar/τ , in agreement with the uncertainty principle.

ACKNOWLEDGMENTS

This research was supported by the U. S. Public Health Service, the National Science Foundation, the Directorate of Chemical Sciences of the U. S. Air Force Office of Scientific Research, and the Petroleum Research Fund of the American Chemical Society. We have also benefited from the use of facilities provided in part by the Advanced Research Projects Agency for materials research at The University of Chicago.